



THE UNIVERSITY *of* EDINBURGH

Edinburgh Research Explorer

## Non-linear dilational rheology of liquid-liquid interfaces stabilized by dipeptide hydrogels

### Citation for published version:

Carbonell Aviñó, F & Clegg, PS 2022, 'Non-linear dilational rheology of liquid-liquid interfaces stabilized by dipeptide hydrogels', *Rheologica acta*, vol. 2023, 62, pp. 45-55. <https://doi.org/10.1007/s00397-022-01380-x>

### Digital Object Identifier (DOI):

[10.1007/s00397-022-01380-x](https://doi.org/10.1007/s00397-022-01380-x)

### Link:

[Link to publication record in Edinburgh Research Explorer](#)

### Document Version:

Peer reviewed version

### Published In:

Rheologica acta

### General rights

Copyright for the publications made accessible via the Edinburgh Research Explorer is retained by the author(s) and / or other copyright owners and it is a condition of accessing these publications that users recognise and abide by the legal requirements associated with these rights.

### Take down policy

The University of Edinburgh has made every reasonable effort to ensure that Edinburgh Research Explorer content complies with UK legislation. If you believe that the public display of this file breaches copyright please contact [openaccess@ed.ac.uk](mailto:openaccess@ed.ac.uk) providing details, and we will remove access to the work immediately and investigate your claim.



# Nonlinear dilational rheology of liquid-liquid interfaces stabilized by dipeptide hydrogels

Fernando Carbonell-Aviñó ·  
Paul S. Clegg

Received: date / Accepted: date

**Abstract** We investigate the effects of salt concentration on the rheological properties of dipeptide hydrogel fibres at liquid-liquid interfaces. The interfaces were subjected to large amplitude oscillatory dilation (LAOD) experiments across a range of oscillation strains and frequencies. Lissajous plots of pressure-strain were used for characterizing the viscoelastic properties and for identifying apparent yielding. We show that key aspects of the rheological response of the interfaces vary significantly with salt concentration. At low strain, independent of salt concentration, Lissajous curves show an almost elliptical shape. As the strain is increased, asymmetry in Lissajous curves evidences a non-linear response. The departure from an ellipse is most obvious at negative strain (at moderate to high salt concentrations) and is suggestive of strain-hardening on compression. The Lissajous curves tilt towards the diagonal at elevated salt concentration demonstrating that the interfaces are becoming increasingly elastic. However, increasing the frequency of the oscillation has little systematic effect. We infer that the addition of salt leads to the development of structure on the interfaces from our observations strain-hardening and of the increasingly elastic response. To fully capture the range of behaviour, we suggest a modification of the analysis to calculate the strain-hardening ratio  $S$  used to quantify the degree of nonlinearities from Lissajous figures, so as to better reveal the presence of instant strain-softening and strain-hardening responses.

**Keywords** Interface · Hydrogel · Peptide

---

School of Physics and Astronomy,  
University of Edinburgh,  
Peter Guthrie Tait Road,  
Edinburgh, EH9 3FD, UK.  
E-mail: paul.clegg@ed.ac.uk

## 1 Introduction

Emulsions are a crucial design motif for food, personal care, home care and agrochemical products. (Tan and McClements, 2021; Taylor, 1998) To prevent the liquid droplets in the emulsion from coalescing the liquid-liquid interfaces must remain stable during collisions. Furthermore, the detailed flow properties of these interfaces may enhance the droplet lifetime by also suppressing ripening. (Bos and Vliet, 2001; Dickinson, 2001; Bantchev and Schwartz, 2003) Long sticky fibres, of nano-scale width, constitute a novel coating for interfaces; the mechanical properties of the interfaces remain to be thoroughly investigated.

It is well-known that some short sequences of peptides can form hydrogels at low concentration. (Jayawarna et al., 2006; Mahler et al., 2006) These molecules and the resulting hydrogels are increasingly being investigated for their capabilities as emulsifiers. Early work on emulsification (and film and foam formation) involved using dipeptides with a protecting group at one end of the molecule (see Figure 1, inset). (Johnson et al., 2010; Li et al., 2014; Bai et al., 2014; Fleming et al., 2014) An alternative approach, which is becoming increasingly popular, is to avoid this protecting group (Scott et al., 2016; Moreira et al., 2017; Wychowaniec et al., 2020) or to modify it to enhance the emulsification performance. (Moreira et al., 2017; Lv et al., 2019) The latter can lead to high performance molecules which are robust when faced with high temperatures or salt concentrations. (Lv et al., 2019; De Leon Rodriguez and Hemar, 2020) Peptide based emulsifiers also permit a higher level of functionality due to the possibility of triggering or disabling the interfacial activity via the use of an enzyme. (Moreira et al., 2016, 2017; Castelletto et al., 2019) Longer peptide sequences with switchable interfacial properties have also been explored. (Dexter et al., 2006; Dexter and Middelberg, 2007)

Previous investigations have shown that a tangle of hydrogel fibres exist at the interface. (Li et al., 2014) This indicates that the stability of droplets and bubbles is due to a complex composite rather than individual interfacially active molecules. We are interested in the detailed mechanical properties of these composite interfaces so for simplicity, we focus on the canonical simple molecule naphthalene protected diphenylalanine (2NapFF, Figure 1, inset). (Chen et al., 2010; Li et al., 2016; Avino et al., 2017) We induce gelation via the addition of a salt; the choice of salt has a profound influence on the properties of the 2NapFF hydrogel in bulk. (Chen et al., 2011)

The study of the rheological properties of complex interfaces involves the imposition of small area (dilatational rheology) and shape (shear rheology) variations, typically at a known frequency. (Miller et al., 1996; Sagis, 2011; Erni, 2011; Sagis and Fischer, 2014) Here we are interested in the mechanical properties of an interfacial layer and we carry out dilatational rheology of an interface using a pendant drop. The volume of the droplet is oscillated at a fixed frequency and the shape of the droplet is measured. By fitting the Young-Laplace equation to the droplet shape both the imposed change in area (i.e. the strain) and the surface pressure response are measured. A good correspondence between the Young-Laplace equation and the droplet shape

is essential. (Nagel et al., 2017) A sweep of the strain amplitude is usually conducted as a first step to determine the critical strain value beyond which the behaviour of the interface becomes non-linear. (van Kempen et al., 2013) Once this is known, the properties of the interface can be further interrogated by applying frequency sweeps in the linear and/or non-linear regimes.

In Refs. (Rühs et al., 2013a,b; van Kempen et al., 2013), Lissajous plots were employed to analyse amplitude sweeps for interfacial dilatational rheology studies. Strain moduli characteristic of the full plot were developed to draw out quantitative details from the data. While this works excellently under many circumstances, contradictions are known to occur whereby the data from a strain softening material appear to indicate strain hardening on a Lissajous plot. (Mermet-Guyennet et al., 2015)

In this paper, the effect of salt concentration on the mechanical properties of interfaces stabilized by dipeptide fibres is investigated by imposing large amplitude oscillatory dilatational (LAOD) deformations on interfaces using a drop profile tensiometer. We find that non-linearities appear at intermediate and high strain amplitudes, while frequency does not have a significant influence. Interfaces prepared at intermediate salt concentrations, exhibit a viscoelastic response. At the highest salt concentration, interfaces are elastic but yield at low deformations, implying that they have become brittle. Finally, we suggest a modification of the analysis for quantifying non-linearities from Lissajous plots, based on instantaneous strain moduli, to better reveal the presence of strain-softening and strain-hardening responses.

## 2 Experimental

### 2.1 Materials

The 2NapFF dipeptides were synthesized at the University of Glasgow as described elsewhere. (Chen et al., 2010) The solvents and chemicals were purchased from Sigma-Aldrich. Isopropyl myristate (Sigma-Aldrich  $\geq 98\%$  pure) was filtered three times through alumina powder (Honeywell, Aluminium Oxide, activated, basic, Brockmann I) prior to use in order to remove polar impurities. A solution of 100 mL (1M) magnesium sulphate was dissolved in water and used as aliquots. Millipore water (resistivity 18.2 M $\Omega$  cm) was used throughout. For pendant drop experiments water was degassed by heating and stirring under reduced pressure for one hour to avoid bubbles disrupting oscillations.

### 2.2 Methods

Samples were prepared in 20 mL glass vials by adding 10 mM of NaOH to 10 mL of degassed water to achieve a pH  $11 \pm 0.5$  measured with a Seven Easy pH probe (Mettler Toledo AG). 2NapFF dipeptides (0.01 wt%) were then added

on top of the basic solution and dispersed by placing the vial sealed with film (Parafilm) in an ultrasonic bath for 0.5 hours until a translucent slightly viscous solution was formed. After this, the sample was then left to cool to room temperature (22°C) before being transferred to a  $36 \times 36 \times 30 \text{ mm}^3$  glass cuvette.

*Apparatus validation* The droplet volume influences the accuracy of the pendant drop tensiometer (Krüss Easy Drop, Krüss GmbH, Germany) because spherical droplets yield inconsistent results. (Hoorfar and Neumann, 2006) To avoid this, we increased the volume of the oil droplet until the interfacial tension of the bare interface equilibrated to a value of 29 mN/m which compares favourably with literature values. (Binks et al., 2010) The final volume was 25  $\mu\text{L}$ . The second stage-gate is the quality of the fit to the Young-Laplace equation. After optimisation is complete, the software shows the mean squared deviation of the profile from the fit to the model. A high fit error, in the range of tens or hundreds of microns, is associated with solidifying interfaces, where wrinkles are observed in compressed interfacial films. (Hegemann et al., 2018) A clean isopropyl myristate/water interface gives a fit error  $< 1 \mu\text{m}$  and thus experiments with fit errors  $\geq 1 \mu\text{m}$  were rejected. Next, we verify that the subphase contributions do not dominate over interfacial stresses by calculating the Boussinesq number (Erk et al., 2012; Brenner, 2013; Mears, 2020) using  $Bq = E/\omega\nu L$ . For the smallest interfacial dilational modulus  $E = 0.05 \text{ mN/m}$ , and the highest frequency = 0.2 Hz we find a  $Bq > 10^2$  (for the drop length scale  $L = 1 \text{ mm}$  with the viscosity of isopropyl myristate as  $\nu = 1.02 \text{ mPa s}$  at 20°C) indicating the interfacial dilational elasticity dominates.

*Experiment setup* After a deep cleaning of the instrument parts with hexane, followed by methanol and rinsing with Millipore water, the instrument was tested by placing Millipore water in the cuvette and forming an air bubble with a J-shaped needle to achieve an interfacial tension of  $72 \pm 0.5 \text{ mN/m}$  at 22°C. Next, the syringe was filled with isopropyl myristate and a droplet of 25  $\mu\text{L}$  formed with interfacial tension comparable to  $\gamma = 29 \pm 0.5 \text{ mN/m}$  at 22°C. Then the water in the cuvette was replaced by the basic solution of dispersed dipeptides. To equilibrate the solution, we again form the oil droplet and let it rest ( $\approx 5$  minutes);  $\gamma$  drops rapidly ( $< 1$  second) from  $\approx 29 \text{ mN/m}$  to  $\approx 25 \text{ mN/m}$  (data not shown). Now aliquots of different salt concentrations (0.1 mg/mL, 0.2 mg/mL, 0.3 mg/mL and 0.4 mg/mL) were added on top of the sample to induce film gelation. Finally, the cuvette was covered with a lid to minimise evaporation.

The surface tension of an interfacial film from a static droplet was measured before, during and after the addition of salt and left until the sample reached equilibrium ( $\approx 5$  hours). Then the surface tension was recorded during amplitude and frequency sweep experiments to study the non-linear response of the complex interfaces. During the sweep tests, sinusoidal oscillations with a strain amplitude and frequency that increased from 1.5% to 25% and 0.02 Hz to 0.2 Hz respectively were performed. The experiments consisted of 20 cycles

of oscillations with 5 minutes rest between experiments. The initial and final cycles were removed from the analysis to eliminate the influence of potential outliers. Outliers were also removed from the raw data in both axis ( $x$ ,  $y$ ) and smoothing was carried out via a running average of point pairs.

### 2.3 Describing the data

Outside the linear regime, physical meaning can be extracted from the Lissajous plots formed by plotting the pressure as a function of strain. For a perfect elastic solid, the Lissajous plot shows a straight line, for a pure viscous response a perfect circle is found and for a linear viscoelastic fluid the plot is an ellipse. Such plots have been used in bulk LAOS experiments to study the rheological properties of viscoelastic materials in the nonlinear regime including, polymer solutions (Philippoff, 1966), creams (Davis, 1971) and clay-water systems (Payne and Whittaker, 1971; Krizek, 1971). Ewoldt *et al.* (Ewoldt *et al.*, 2008) introduced a set of elastic moduli in order to quantify the response of nonlinear viscoelastic materials at large shear strains. To characterize non-linearities distorting the ellipse, these authors defined the shear strain-hardening ratio  $S$  where  $S < 0$  indicates strain-softening,  $S > 0$  implies strain-hardening and  $S = 0$  denotes an elastic response. Ewoldt's approach to calculate the  $S$ -factor, was later extended by others (van Kempen *et al.*, 2013; Rühls *et al.*, 2013a) to characterize the response of air-water interfaces in LAOD deformations. Here the pressure is defined as:

$$\Pi = \gamma - \gamma_0 \quad (1)$$

where  $\gamma$  is the tension of the interface and  $\gamma_0$  is the tension of the non deformed interface. Due to the asymmetry in the Lissajous plots during a full cycle, the strain-hardening ratio  $S$  is defined for both extension and compression as:

$$S_{ext} \equiv \frac{E_{L,E} - E_{M,E}}{E_{L,E}} \quad (2)$$

$$S_{com} \equiv \frac{E_{L,C} - E_{M,C}}{E_{L,C}} \quad (3)$$

where  $E_{L,E}$  and  $E_{M,E}$  is the large and minimum strain modulus upon extension and  $E_{L,C}$  and  $E_{M,C}$  upon compression (see Ref. (van Kempen *et al.*, 2013), Fig. 2).

## 3 Results and Discussion

The interfacial tension  $\gamma$  of interfaces stabilized by dipeptide fibres (2NapFF) at 0.2 mg/mL and 0.3 mg/mL magnesium sulfate was measured first during dipeptide adsorption and subsequently after the addition of salt. Here the quantities of dipeptide are small compared to those required to create a bulk

hydrogel. In the absence of salt, spherical micelles are expected at 0.01 wt% 2NapFF. (Cardoso et al., 2016) The addition of salt leads to both the formation of fibres and, potentially, gelation on the interface. (Li et al., 2014; Avino et al., 2017)  $\gamma$  for a isopropyl myristate-milli-Q water interface is  $\approx 29.7$  mN/m at 22°C and decreases to  $\approx 25$  mN/m due to the presence of dipeptide. After addition of salt,  $\gamma$  decreases slowly to  $\approx 16.5$  mN/m and  $\approx 13.5$  mN/m for interfaces prepared at 0.2 mg/mL and 0.3 mg/mL respectively, Figure 1. After 5 h, interfaces reach equilibrium and are ready for oscillation.

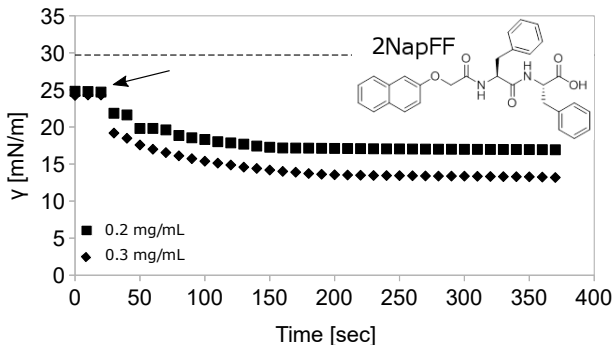


**Fig. 1** Interfacial tension,  $\gamma$ , of interfaces prepared using 0.01 wt% 2NapFF. Oil droplets are left unperturbed until the interfacial tension reaches equilibrium. The black arrow indicates the addition of salt. The dashed line is  $\gamma$  of a clean isopropyl myristate-milliQ water interface. Inset: Naphthalene dipeptide molecules used in this study.

### 3.1 Lissajous plots

The effect of salt on the mechanical properties of oil-water interfaces stabilized by dipeptide fibres (2NapFF), was investigated by imposing large amplitude oscillatory dilatational (LAOD) frequency and strain sweeps on the oil droplets. We begin by looking at the low salt case as our baseline for comparison. The surface pressure of interfaces prepared at 0.1 mg/mL magnesium sulfate oscillated at 0.02 Hz and 1.5% strain is below the detection limit of the apparatus (see Figure 2a). At higher strain (8%), the data is still a bit scattered in the plateau region of the pressure-strain curve, however, the curve is a horizontal ellipse indicative of a viscous interface (Figure 2b). With increasing frequency (Figure S1), the noise decreases and lissajous ellipses become wider and slightly tilted, characteristic of the interfaces becoming increasingly viscoelastic.

At 16% lissajous curves become asymmetric due to a noticeably non-linear response from the interfaces (see Figure 2c). At positive strains, the curve remains indicative of viscous flow. Intiguently, we observe secondary oscillations (see black arrow in Figure 2c) corresponding to several distinct strains being

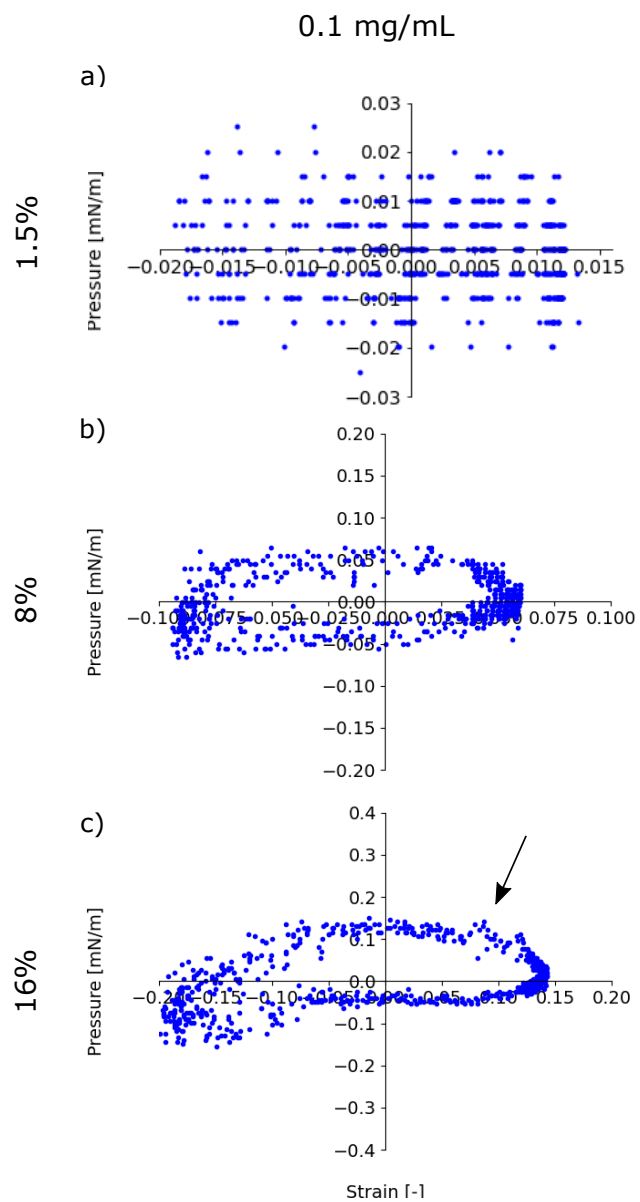


**Fig. 2** Lissajous plots obtained during amplitude sweeps (a) 1.5%, (b) 8% and (c) 16% of an interface made of 0.01 wt% 2NapFF prepared at 0.1 mg/mL magnesium sulfate, oscillated at a fixed frequency (0.02 Hz). Black arrow indicates secondary oscillations.



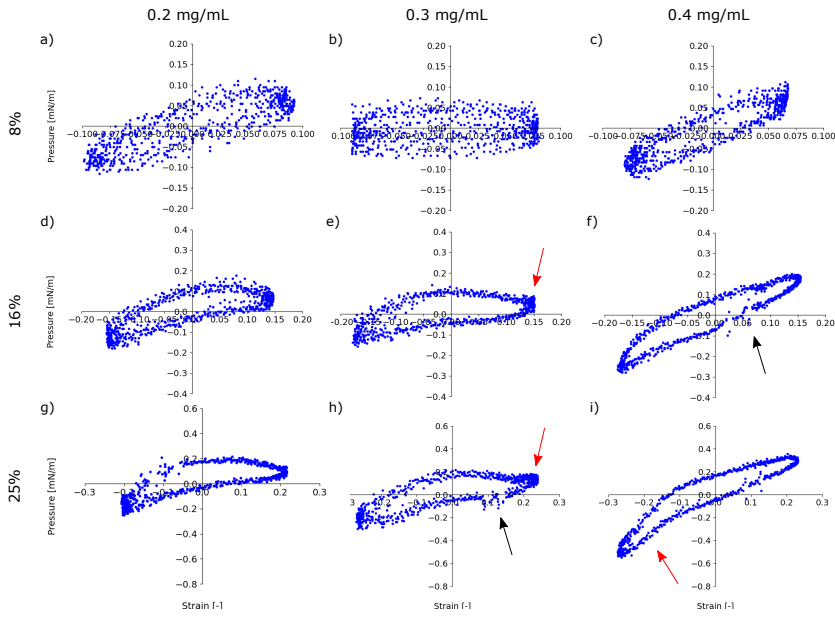


**Fig. 3** Lissajous plots obtained during amplitude sweeps (8–25%) of interfaces made of 0.01 wt% 2NapFF prepared at different salt concentrations (0.2–0.4 mg/mL), oscillated at a fixed frequency (0.02 Hz). Black and red arrows indicate secondary oscillations and strain-hardening respectively.

associated with the same pressure; this has previously been observed in interfacial rheology studies (see Figure 10 in Ref. (Sagis et al., 2014)). At negative strains, there is a noticeable start of an asymmetric response, suggestive of strain-hardening on compression. This evidences increasing structure on the interface. Lissajous curves from interfaces oscillated at higher frequencies (Figure S2), share similarities with Figure 2c but, they become wider and more tilted with increasing frequency. At the highest frequency irregular fluctuations come to dominate (Figure S2).

Next we consider the effect of increasing the salt concentration. Figure 3 shows the lissajous curves of interfaces prepared at (left panel) 0.2 mg/mL, (middle panel) 0.3 mg/mL and (right panel) 0.4 mg/mL magnesium sulfate oscillated at 0.02 Hz and (first row) 8%, (second row) 16% and (third row) 25% strain. At 8% strain (Figures 3a,b,c) all Lissajous curves are quite noisy but show a close to perfect ellipse, suggesting they reflect linear response. Interfaces oscillated at 16% and 25% show relatively horizontal major axes at salt concentrations 0.2 mg/mL and 0.3 mg/mL with the major axis tilting closer to the diagonal for 0.4 mg/mL (Figures 3d-i). This tilting corresponds to an increase in the elastic response clearly indicating that at elevated salt concentration there is interfacial structure that resists extension. It is noticeable that both Figure 3a and Figure 3c are also somewhat tilted.

At first sight, Figures 3d, e, g and h are reminiscent of the low salt case presented in Figure 2b, c, however, there is strain-softening on extension when

beginning from maximum compression and an onset of strain-hardening approaching the maximum extension at 0.3 mg/mL (red arrows, Figures 3e, h). By contrast, there is more pronounced strain-hardening on compression at 0.4 mg/mL (most clearly in Figure 3i). Here, the maximum surface pressure observed on compression is significantly higher than that for extension. Secondary oscillations are visible on compression in both Figures 3f, h (black arrows).

Interfaces oscillated at higher frequencies (Figures S3), do not lose the elliptical shape when deformed at 8%, but become wider and more tilted, which indicates interfaces with higher viscoelastic moduli. At 16% strain, the pressure increases with increasing frequency for interfaces prepared at 0.2 mg/mL, but barely changes the shape of the Lissajous curves (Figure S4a,b). On the other hand, at higher salt concentrations (Figure S4c-g), the increase in frequency seems to have a greater effect. At 0.3 mg/mL and 0.4 mg/mL the pressure increases in extension and in compression, hence forming wider Lissajous curves. For 25% (Figures S5), the increase in frequency only has a modest affect on the shape of the Lissajous curves. Across all frequencies and most amplitudes, we see a strain-hardening kink on extension at 0.3 mg/mL which gives way to a more tilted ellipse and more profound strain-hardening on compression at 0.4 mg/mL. These trends show that the addition of salt leads to the development of structure on the interface which contributes a marked strain-hardening aspect to the response.

### 3.2 Quantifying the degree of non-linearities from Lissajous plots

Non-linearities in Lissajous plots can be quantified using the strain-hardening ratio  $S$  ( $S$ -factor), equations 2 and 3. An  $S$ -factor with a value close to zero is indicative of interfaces with linear elastic response; negative or positive values correspond to strain-softening or strain-hardening responses respectively. Figure 4a shows the  $S$ -factor of Lissajous plots for the interface prepared at 0.1 mg/mL (Figure 2) with the scattered data for the lowest amplitude suppressed. At 8% strain, the  $S$ -factor is positive and increases in extension and in compression with increasing strain amplitude, implying a strain-hardening response.

The  $S$ -factor of Lissajous plots for interfaces prepared at 0.2–0.4 mg/mL (Figure 3) is presented in Figure 4b,c,d. At 0.2 mg/mL the  $S$ -factor is negative on extension at 8% and 16%, but becomes positive at 25%, which suggests an interface with a strain-softening response at low and intermediate deformations and with a strain-hardening response at higher deformations. In compression, we observe a positive  $S$ -factor increasing non-monotonically, being close to zero at 8% and reaching its maximum value at 16%. At 25% this decreases slightly implying that, the strain-hardening response decreases at high deformations after reaching its maximum value at intermediate deformations. The  $S$ -factor from the interface prepared at 0.3 mg/mL oscillated at 8% was not calculated because the noise was still too high even after smoothing the data.

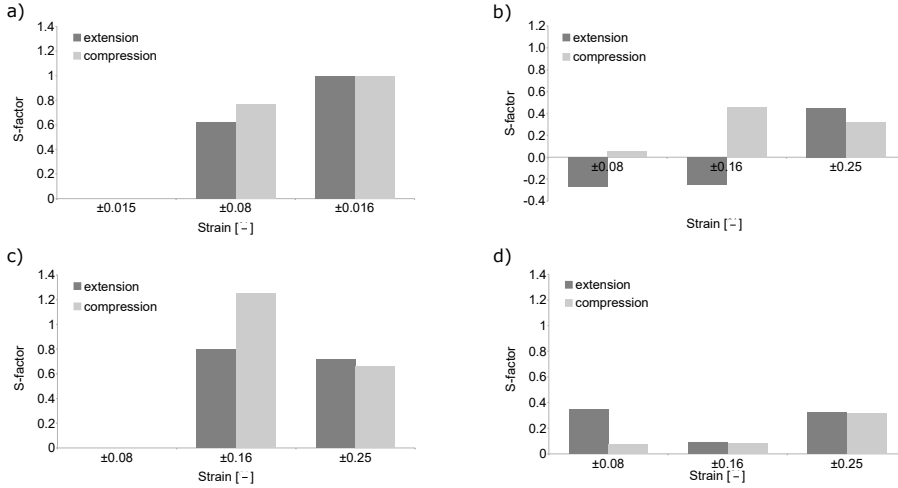


**Fig. 4**  $S$ -factor obtained from Lissajous plots during amplitude sweeps (1.5–25%) of interfaces made from 0.01 wt% 2NapFF prepared at (a) 0.1 mg/mL and (b) 0.2 mg/mL, (c) 0.3 mg/mL, (d) 0.4 mg/mL magnesium sulfate, oscillated at a fixed frequency (0.02 Hz). A  $S$ -factor with a value close to zero indicates an interface with an elastic response, whereas a  $S$ -factor with a positive or negative value corresponds to an interface with a strain-hardening and strain-softening response respectively.

At 16%, the  $S$ -factor is positive on extension and compression and decreases slightly for interfaces oscillated at 25%, indicating an interface with a higher strain-hardening response in extension and compression at intermediate deformations. Lastly, Lissajous curves from interfaces prepared at 0.4 mg/mL, show a positive but low  $S$ -factor in extension and in compression. In extension, this is higher in interfaces oscillated at 8% and 25%, suggesting a less strain-hardening interface at intermediate deformations. However, in compression, the  $S$ -factor is close to zero in extension at 8% and 16% and increases at 25%, implying an interface with an elastic response at low and intermediate deformations in compression.

Analysing the  $S$ -factor, we find that this contradicts the Lissajous curves to some extent. Peak strain-hardening is shown at 0.1 and 0.3 mg/ml (Figure 4) in contrast to the relatively monotonic evolution of the Lissajous curves. Furthermore, Lissajous plots show some strain-softening in extension for interfaces oscillated at 16% and 25%, which is particularly clear when starting from maximum compression, the  $S$ -factor is often positive. This phenomena was first reported by Ma *et al.* (Ma *et al.*, 1999) when studying the micro-mechanical properties of a keratin filament network, using strain-controlled rheometry. However, it was not until Ewoldt *et al.* (Ewoldt *et al.*, 2008) introduced a framework to interpret non-linearities physically in the response to imposed LAOS deformations, that this issue was raised. In this work they focus on the local behaviour represented by the Lissajous curves and hence systems are reported to be strain-hardening. Subsequently Mermet-Guyennet *et al.* (Mermet-Guyennet *et al.*, 2015) realized that, even if the viscoelastic

modulus decreases in the non-linear regime with increasing deformation for a large number of soft materials, they still are usually reported as showing a strain-hardening response when analyzed via Lissajous curves. They called this phenomena the strain-softening/strain-hardening paradox after demonstrating that the strain-hardening response observed is local due to the use of a tangent modulus in the LAOS analysis that increases with increasing deformation and by showing that the strain-softening is the dominant effect, and hence the overall response as shown by the change in slope of the minimum strain modulus  $G_M$ .

### 3.3 New approach to quantify non-linearities

In the previous Section we addressed the differences between the Lissajous plots from Figures 2 and 3 and the  $S$ -factor from Figure 4. Here, we suggest a modification to the analysis to quantify non-linearities from Lissajous plots that reveals better the presence of strain-softening and strain-hardening responses. We replace the minimum strain modulus  $E_M$  in Equations 2 and 3 by the slope of the instantaneous strain modulus  $E$  sampled at a subset of points (here alternate points from a single cycle) to give,

$$s_{ext} \equiv \frac{E - E_{L,E}}{E_{L,E}} \quad (4)$$

$$s_{com} \equiv \frac{E - E_{L,C}}{E_{L,C}} \quad (5)$$

The signs in the numerator have been chosen to preserve the interpretation of the sign of the  $s$ -factor. Figure 5 shows the evolution of the  $s$ -factor of Lissajous curves from interfaces prepared at 0.2 mg/mL, 0.3 mg/mL and 0.4 mg/mL magnesium sulfate oscillated at a frequency of 0.05 Hz and 16% strain.

The  $s$ -factor from a Lissajous curve of an interface prepared at 0.2 mg/mL in extension, is positive at negative strains (Figure 5a). These results indicate that at the start of extension the interface shows an initial strain-hardening response, however, this becomes strain-softening as the strain increases. In compression, the interface shows a more elastic response, observed by the  $s$ -factor barely changing and being close to zero.

The evolution of the  $s$ -factor from a Lissajous plot of an interface prepared at 0.3 mg/mL (Figure 5b) is somewhat similar. The  $s$ -factor for extension is positive at negative strains, but decreases fast with increasing strain. At a strain near zero, this reaches zero and decreases further until a strain  $\approx +0.08$ , where it reaches its minimum value. At higher strains, the  $s$ -factor increases and becomes strain-hardening by the end of extension. In compression, the  $s$ -factor is more varied than that for an interface prepared at 0.2 mg/mL with an overall tendency towards strain-softening.

At 0.4 mg/mL, the  $s$ -factor again starts positive in extension (Figure 5c), however, the values are far lower than for interfaces prepared at 0.2 mg/mL

and 0.3 mg/mL. This suggests that the interface prepared at 0.4 mg/mL has a more elastic response than interfaces prepared at lower salt concentrations. Similar to interfaces prepared at 0.3 mg/mL, the *s-factor* increases and becomes slightly positive by the end of extension. In compression, the *s-factor* barely changes and is close to zero. Overall, Figure 5 shows a more clear progression with salt concentration and a more realistic reflection of the Lissajous curves.

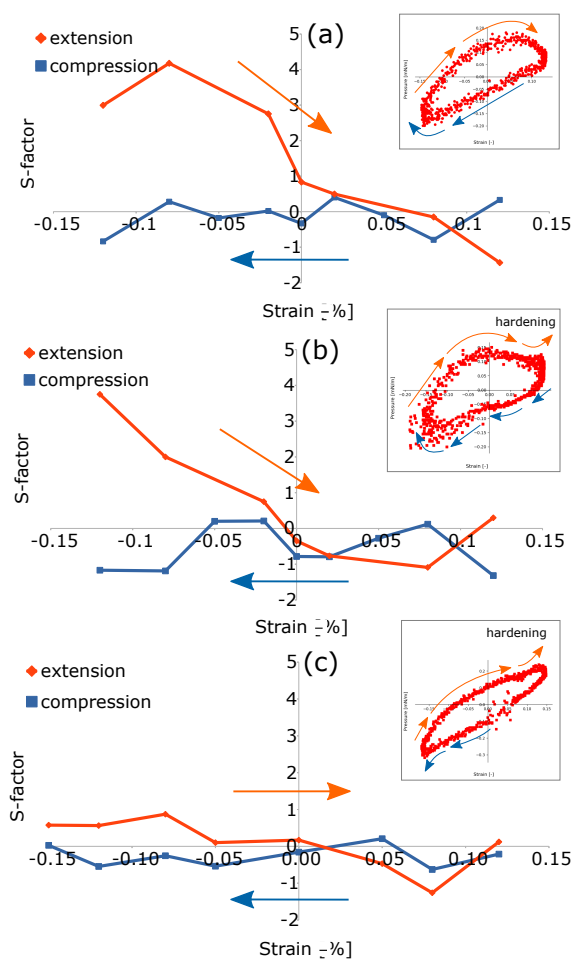


**Fig. 5** Evolution of the *s-factor* from Lissajous plots of interfaces made of 0.01 wt% 2NapFF oscillated at 0.05 Hz and 16%, prepared at (a) 0.2 mg/mL, (b) 0.3 mg/mL and (c) 0.4 mg/mL magnesium sulfate. The arrows indicate the direction of the cycle (expansion and compression). Insets show Lissajous plots of interfaces being characterized. The arrows in insets are placed to aid the eye with the interface response and to indicate the direction of the cycle. This form of analysis emphasises the steady evolution of the interfacial properties with increasing salt concentration.

## 4 Conclusions

In this paper we have investigated the effect of salt concentration on the rheological properties of salt-induced hydrogel films made of 2NapFF. Interfaces were subjected to strain and frequency sweeps in the linear and non-linear viscoelastic regime via the oscillating drop technique. Plotting pressure-strain curves from interfaces subjected to LAOD deformations as Lissajous curves has allowed us to analyse the rheological response of the interfaces beyond the linear regime.

All interfaces showed Lissajous curves with an almost elliptical shape at 8% strain, which indicates that these are still within the linear regime. Asymmetric Lissajous curves from 16% strain indicates that the interfaces are now in the non-linear regime. This is most noticeable, at negative strains, where the shape is suggestive of strain-hardening on compression. This evidences increasing structure on the interface. Interfaces prepared at 0.4 mg/mL salt showed the highest elastic response of all interfaces, with the pressure still increasing after these have yielded and very pronounced strain hardening on compression (especially at 25% strain). By contrast, increasing the frequency did not have a significant effect on the properties of the interfaces compared to the strain. From the increasingly elastic character and the strain-hardening response, we infer that the addition of salt leads to the development of structure on the interface.

Finally, we and other authors (Mermet-Guyennet et al., 2015; Giménez-Ribes et al., 2020; Precha-Atsawan et al., 2018) realized that the strain-hardening ratio  $S$  or  $S$ -factor used to quantify non-linearities from Lissajous plots, can sometimes give misleading measures. We suggest using the instantaneous-strain elastic moduli  $E$  rather than the minimum-strain elastic moduli  $E_M$  in Equations 2 and 3, to capture the overall response of the interfaces, regardless of which response (elastic or viscous) dominates.

**Acknowledgements** FC-A gratefully acknowledges a studentship funded by the EPSRC (EP/N509644/1). We thank D.J. Adams for providing the 2NapFF dipeptides. For the purpose of open access, the author has applied a Creative Commons Attribution (CC BY) licence to any Author Accepted Manuscript version arising from this submission.

## Conflict of interest

The authors declare that they have no conflict of interest.

Supporting Information file contains additional figures of Lissajous plots from interfaces oscillated at higher frequencies (0.05 Hz, 0.1 Hz and 0.2 Hz).

## References

- Avino F, Matheson AB, Adams DJ, Clegg PS (2017) Long-lived foams stabilized by a hydrophobic dipeptide hydrogel. *Organic & Biomolecular Chemistry* 15:6342–6348
- Bai S, Pappas C, Debnath S, Frederix PW, Leckie J, Fleming S, Ulijn RV (2014) Stable emulsions formed by self-assembly of interfacial networks of dipeptide derivatives. *ACS Nano* 8:7005–7013
- Bantchev GB, Schwartz DK (2003) Surface shear rheology of  $\beta$ -casein layers at the air/solution interface: Formation of a two-dimensional physical gel. *Langmuir* 19:2673–2682
- Binks BP, Fletcher PD, Holt BL, Parker J, Beaussoubre P, Wong K (2010) Drop sizes and particle coverage in emulsions stabilised solely by silica nanoparticles of irregular shape. *Physical Chemistry Chemical Physics* 12:11967–11974
- Bos MA, Vliet TV (2001) Interfacial rheological properties of adsorbed protein layers and surfactants: a review. *Advances in Colloid and Interface Science* 91:437–471
- Brenner H (2013) *Interfacial transport processes and rheology*. Elsevier, Amsterdam
- Cardoso AZ, Mears LL, Cattoz BN, Griffiths PC, Schweins R, Adams DJ (2016) Linking micellar structures to hydrogelation for salt-triggered dipeptide gelators. *Soft Matter* 12:3612–3621
- Castelletto V, Edwards-Gayle CJ, Hamley IW, Barrett G, Seitsonen J, Ruokolainen J (2019) Peptide-stabilized emulsions and gels from an arginine-rich surfactant-like peptide with antimicrobial activity. *ACS Applied Materials & Interfaces* 11:9893–9903
- Chen L, Revel S, Morris K, Serpell LC, Adams DJ (2010) Effect of molecular structure on the properties of naphthalene-dipeptide hydrogelators. *Langmuir* 26:13466–13471
- Chen L, Pont G, Morris K, Lotze G, Squires A, Serpell LC, Adams DJ (2011) Salt-induced hydrogelation of functionalised-dipeptides at high pH. *Chemical Communications* 47:12071–12073
- Davis SS (1971) Viscoelastic properties of pharmaceutical semisolids iv: Destructive oscillatory testing. *Journal of pharmaceutical sciences* 60:1356–1360
- De Leon Rodriguez LM, Hemar Y (2020) Prospecting the applications and discovery of peptide hydrogels in food. *Trends in Food Science & Technology* 104:37–48
- Dexter AF, Middelberg AP (2007) Switchable peptide surfactants with designed metal binding capacity. *The Journal of Physical Chemistry C* 111:10484–10492
- Dexter AF, Malcolm AS, Middelberg AP (2006) Reversible active switching of the mechanical properties of a peptide film at a fluid–fluid interface. *Nature Materials* 5:502–506

- Dickinson E (2001) Milk protein interfacial layers and the relationship to emulsion stability and rheology. *Colloids and Surfaces B: Biointerfaces* 20:197–210
- Erk KA, Martin JD, Schwalbe JT, Phelan FR Jr, Hudson SD (2012) Shear and dilational interfacial rheology of surfactant-stabilized droplets. *Journal of Colloid and Interface Science* 377:442–449
- Erni P (2011) Deformation modes of complex fluid interfaces. *Soft Matter* 7:7586–7600
- Ewoldt RH, Hosoi A, McKinley GH (2008) New measures for characterizing nonlinear viscoelasticity in large amplitude oscillatory shear. *Journal of Rheology* 52:1427–1458
- Fleming S, Debnath S, Frederix PW, Hunt NT, Ulijn RV (2014) Insights into the coassembly of hydrogelators and surfactants based on aromatic peptide amphiphiles. *Biomacromolecules* 15:1171–1184
- Giménez-Ribes G, Habibi M, Sagis LM (2020) Interfacial rheology and relaxation behavior of adsorption layers of the triterpenoid saponin escin. *Journal of Colloid and Interface Science* 563:281–290
- Hegemann J, Knoche S, Egger S, Kott M, Demand S, Unverfehrt A, Rehage H, Kierfeld J (2018) Pendant capsule elastometry. *Journal of Colloid and Interface Science* 513:549–565
- Hoorfar M, Neumann A (2006) Recent progress in axisymmetric drop shape analysis (adsa). *Advances in Colloid and Interface Science* 121:25–49
- Jayawarna V, Ali M, Jowitt TA, Miller AF, Saiani A, Gough JE, Ulijn RV (2006) Nanostructured hydrogels for three-dimensional cell culture through self-assembly of fluorenylmethoxycarbonyl-dipeptides. *Advanced Materials* 18:611–614
- Johnson EK, Adams DJ, J CP (2010) Directed self-assembly of dipeptides to form ultrathin hydrogel membranes. *Journal of the American Chemical Society* 132:5130–5136
- van Kempen SE, Schols HA, van der Linden E, Sagis LM (2013) Non-linear surface dilatational rheology as a tool for understanding microstructures of air/water interfaces stabilized by oligofructose fatty acid esters. *Soft Matter* 9:9579–9592
- Krizek RJ (1971) Rheologic behavior of clay soils subjected to dynamic loads. *Transactions of the Society of Rheology* 15:433–489
- Li T, Kalloudis M, Cardoso AZ, Adams DJ, Clegg PS (2014) Drop-casting hydrogels at a liquid interface: The case of hydrophobic dipeptides. *Langmuir* 30:13854–13860
- Li T, Nudelman F, Tavaicoli JW, Vass H, Adams DJ, Lips A, Clegg PS (2016) Long-lived foams stabilized by a hydrophobic dipeptide hydrogel. *Advanced Materials Interfaces* 3:1500601
- Lv W, Hu T, Taha A, Wang Z, Xu X, Pan S, Hu H (2019) Lipo-dipeptide as an emulsifier: Performance and possible mechanism. *Journal of Agricultural and Food Chemistry* 67:6377–6386
- Ma L, Xu J, Coulombe PA, Wirtz D (1999) Keratin filament suspensions show unique micromechanical properties. *Journal of Biological Chemistry*



- 274(27):19145–19151
- Mahler A, Reches M, Rechter M, Cohen S, Gazit E (2006) Rigid, self-assembled hydrogel composed of a modified aromatic dipeptide. *Advanced Materials* 18:1365–1370
- Mears R (2020) Structure and mechanical properties of model colloids at liquid interfaces. The University of Edinburgh
- Mermet-Guyennet M, Gianfelice de Castro J, Habibi M, Martzel N, Denn M, Bonn D (2015) Laos: The strain softening/strain hardening paradox. *Journal of Rheology* 59:21–32
- Miller R, Wüstneck R, Krägel J, Kretzschmar G (1996) Dilational and shear rheology of adsorption layers at liquid interfaces. *Colloids and Surfaces A: Physicochemical and Engineering Aspects* 111:75–118
- Moreira IP, Sasselli IR, Cannon DA, Hughes M, Lamprou DA, Tuttle T, Ulijn RV (2016) Enzymatically activated emulsions stabilised by interfacial nanofibre networks. *Soft Matter* 12:2623–2631
- Moreira IP, Piskorz TK, van Esch JH, Tuttle T, Ulijn RV (2017) Biocatalytic self-assembly of tripeptide gels and emulsions. *Langmuir* 33:4986–4995
- Nagel M, Tervoort TA, Vermant J (2017) From drop-shape analysis to stress-fitting elastometry. *Advances in Colloid and Interface Science* 247:33–51
- Payne A, Whittaker R (1971) Low strain dynamic properties of filled rubbers. *Rubber chemistry and technology* 44:440–478
- Philippoff W (1966) Vibrational measurements with large amplitudes. *Transactions of the Society of Rheology* 10:317–334
- Precha-Atsawan S, Uttapap D, Sagis LM (2018) Linear and nonlinear rheological behavior of native and debranched waxy rice starch gels. *Food Hydrocolloids* 85:1–9
- Rühs PA, Affolter C, Windhab EJ, Fischer P (2013a) Shear and dilatational linear and nonlinear subphase controlled interfacial rheology of  $\beta$ -lactoglobulin fibrils and their derivatives. *Journal of Rheology* 57:1003–1022
- Rühs PA, Scheuble N, Windhab EJ, Fischer P (2013b) Protein adsorption and interfacial rheology interfering in dilatational experiment. *The European Physical Journal Special Topics* 222:47–60
- Sagis L (2011) Dynamic properties of interfaces in soft matter: Experiments and theory. *Reviews of Modern Physics* 83:1367–1403
- Sagis L, Fischer P (2014) Nonlinear rheology of complex fluid–fluid interfaces. *Current Opinion in Colloid and Interface Science* 19:520–529
- Sagis L, Humblet-Hua K, Van Kempen S (2014) Nonlinear stress deformation behavior of interfaces stabilized by food-based ingredients. *Journal of Physics: Condensed Matter* 26:464105
- Scott GG, McKnight PJ, Tuttle T, Ulijn RV (2016) Tripeptide emulsifiers. *Advanced Materials* 28:1381–1386
- Tan C, McClements DJ (2021) Application of advanced emulsion technology in the food industry: A review and critical evaluation. *Foods* 10:812
- Taylor P (1998) Ostwald ripening in emulsions. *Advances in Colloid and Interface Science* 75:107–163

---

Wychowaniec JK, Patel R, Leach J, Mathomes R, Chhabria V, Patil-Sen Y, Hidalgo-Bastida A, Forbes RT, Hayes JM, Elsayy MA (2020) Aromatic stacking facilitated self-assembly of ultrashort ionic complementary peptide sequence:  $\beta$ -sheet nanofibers with remarkable gelation and interfacial properties. *Biomacromolecules* 21:2670–2680